Time-dependent magnetothermoelastic creep modeling of FGM spheres using method of successive elastic solution

A. Loghman [a,*], S.M.A. Aleayoub [b], M. Hasani Sadi [b]

[a] Department of Mechanical Engineering, Faculty of Engineering, University of Kashan, Kashan, Islamic Republic of Iran
[b] Department of Mechanical Engineering, Islamic Azad University, Arak Branch, Arak, Islamic Republic of Iran

ARTICLE INFO

ABSTRACT

Magnetothermoelastic creep behavior of thick-walled spheres made of functionally graded materials (FGM) placed in uniform magnetic and distributed temperature fields and subjected to an internal pressure is investigated using method of successive elastic solution. The material creep, magnetic and mechanical properties through the radial graded direction are assumed to obey the simple power law variation. Using equations of equilibrium, stress–strain and strain–displacement a differential equation, containing creep strains, for displacement is obtained. A semi-analytical method in conjunction with the Mendelson's method of successive elastic solution has been developed to obtain history of stresses and strains. History of stresses, strains and effective creep strain rate from their initial elastic distribution at zero time up to 55 years are presented in this paper. Stresses, strains and effective creep strain rate are changing in time with a decreasing rate so that after almost 50 years the time-dependent solution approaches the steady state condition when there is no distinction between stresses and strains at 50 and 55 years.

© 2011 Elsevier Inc. All rights reserved.

1. Introduction

In modern technologies a new area concerning the interactions among stress, strain, temperature and electromagnetic fields has been developed. This area which is called magnetothermoelasticity has attracted the researcher's attention due to wide application in geophysics, electrical power engineering, optics and plasma physics. In recent years functionally graded materials are extensively used for structural components working in high temperature environments under mechanical loading and electromagnetic fields. Such components are subjected to creep damage. Time-dependent stress and deformation analysis of these components which gives the history of stresses and deformations is crucial for life assessment of these components. Although in-service examinations of such components gives useful information about the material condition, however history of stresses and deformations are crucial before these information can be used for prediction of the future performance of the component. Therefore time-dependent stress and deformation analysis of such components is very important.

Exact solution for magnetothermoelastic analysis of cylinders and spheres is available in the literature. Magnetothermoelastic problems of FGM cylinders and spheres are studied by Dai and Fu [1] and Ghorbanpour et al. [2]. The thermo-elastic problem of FGM spheres, cylinders and disks has already been analytically studied by Tutuncu and Temel [3]. Yoshihiro and Yoshinobu [4] reported the transient piezothermoelastic analysis for a functionally graded thermopiezoelectric hollow sphere.

* Corresponding author. Tel.: +98 3615912425; fax: +98 3615559930.
E-mail address: aloghman@kashanu.ac.ir (A. Loghman).

Closed form solution for steady state creep problems of FGM cylinders and spheres can be found in the literature.

Creep deformation and stresses in thick-walled cylindrical vessels of FGM subjected to internal pressure was presented by You et al. [5]. They obtained a closed form solution for steady state creep stresses in FGM cylinders. Thermal stresses were not considered and stress redistributions were not presented. Effect of anisotropy on steady state creep in functionally graded cylinders was investigated by Singh and Gupta [6].

Time-dependent creep stress and damage analysis of thick-walled spherical pressure vessels of constant material properties has been investigated by Loghman and Shokouhi [7]. They studied the creep stress and damage histories of thick-walled spheres using the material constant creep and creep rupture properties defined by the Theta projection concept [8]. Loading conditions included an internal pressure and a thermal gradient. Time and temperature dependent response and relaxation of a soft polymer was investigated by Khan and Lopez [9]. Although intensive investigation considering creep of thick-walled spheres and cylinders with constant material properties can be found in the existing literature, Loghman and Wahab [10], Sim and Penny [11], however, little publication can be found dealing with time-dependent creep of FGM spheres and cylinders. Time-dependent deformation and fracture of multi-material systems at high temperature was presented by Xuan et al. [12]. They considered a thick-walled sphere of FGM material subjected to an internal pressure. Using Norton's law for material creep behavior and using equations of equilibrium, compatibility, stress–strain relations and considering the Prandtl–Reuss relations, they obtained a differential equation for the radial stress rate. Radial and circumferential stress distributions with different material creep properties after two hundred hours were illustrated. Yang [13] presented a solution for time-dependent creep behavior of FGM cylinders using Norton's law for material creep constitutive model. Using equations of equilibrium, strain–displacement and stress–strain relations he obtained a differential equation for the displacement rate. There was no exact solution of the equation, however with some simplifications and using Taylor expansion, he obtained the displacement rate and then the stress rates were calculated. When the stress rates were known, the stresses at any time were calculated iteratively.

Recently magnetothermoelastic creep analysis of FGM cylinders has been added to the literature by Loghman et al. [14]. However there is no solution for magnetothermoelastic creep behavior of FGM spheres in the existing literature. The main objective of this paper is to present Time-dependent magnetothermoelastic creep modeling of FGM spheres. The present paper can be used for damage analysis of FGM spheres.

2. Geometry, material properties and loading condition

A hollow FGM sphere with an inner radius r_i and outer radius r_o with perfect conductivity is considered. The sphere is placed in a uniform magnetic field with magnetic intensity vector $\vec{H}(0,0,H_\phi)$ and subjected to an internal pressure P and a distributed temperature field $T = T_0 r^\beta$. Mechanical properties, except Poisson's ratio, through the radial graded direction are assumed to obey the same power law variation as $E = E_0 r^\beta$ and $\alpha = \alpha_0 r^\beta$ where E and α are radial dependent elastic modulus and coefficient of linear expansion and E_0 and α_0 are elastic constants. The radial dependent magnetic permeability, $\mu(r)$ is assumed the same power as mechanical properties $\mu(r) = \mu_0 r^\beta$ where μ_0 is magnetic permeability [H/m]. The uni-axial creep constitutive model is the Norton's law $\dot{\varepsilon}_e^c = B(r)\sigma_e^{n(r)}$ where $\dot{\varepsilon}_e^c$ and σ_e are effective creep strain rate and the effective stress respectively, r is the radial coordinate and $B(r)$ and $n(r)$ are the radial-dependent material creep parameters. In this study $B(r) = b_0 r^{b_1}$ and $n(r)$ is considered to be a constant $n(r) = n_0$. The following data for geometry, material properties [1,5] and loading conditions are used in this study $\frac{r_o}{r_i} = 1.4, E_o = 22$ GPa, $b_o = 0.11 \times 10^{-36}, b_1 = -5, n_0 = 10, \upsilon = 0.3, \alpha_o = 1.2 \times 10^{-6} \frac{1}{°C}, q = \frac{1}{3}, \beta = 2, 1, -1, -2, T_0 = 200 °C, P_i = 100$ MPa, $\mu_0 = 4\pi \times 10^{-7}$ H/m, $H_\phi = 2.23 \times 10^9$ A/m.

3. Basic formulation for magnetothermoelastic creep analysis of FGM spheres

Consider a thick, hollow, FGM sphere with an inner radius r_i and outer radius r_0 subjected to an internal pressure P with perfect conductivity placed in a uniform magnetic $\vec{H}(0,0,H_\phi)$ and a distributed temperature field.

Assuming total strains to be the sum of elastic, thermal and creep strains then the stress–strain relation for spherical symmetry may be written in terms of radial displacement as

$$\sigma_r = c_{11}\frac{\partial u}{\partial r} + 2c_{12}\frac{u}{r} - \lambda_1 T - c_{11}\varepsilon_r^c - 2c_{12}\varepsilon_\theta^c, \tag{1a}$$

$$\sigma_\theta = c_{12}\frac{\partial u}{\partial r} + (c_{11} + c_{12})\frac{u}{r} - \lambda_2 T - c_{12}\varepsilon_r^c - (c_{11} + c_{12})\varepsilon_\theta^c, \tag{1b}$$

$$\lambda_1 = c_{11}\alpha_r + 2c_{12}\alpha_\theta, \tag{1c}$$

$$\lambda_2 = c_{12}\alpha_r + (c_{11} + c_{12})\alpha_\theta, \tag{1d}$$

where $c_{11} = \frac{(1-\upsilon)E}{(1+\upsilon)(1-2\upsilon)}$ and $c_{12} = \frac{\upsilon E}{(1+\upsilon)(1-2\upsilon)}$ and considering $\alpha_r = \alpha_\theta = \alpha$ then $\lambda_1 = \lambda_2 = \frac{E\alpha}{1-2\upsilon}$.

In which E, ν and α are elastic modulus, Poisson's ratio and coefficient of linear expansion respectively. The equilibrium equation of the FGM sphere placed in a uniform magnetic field is

$$\frac{d\sigma_r}{dr} + \frac{2(\sigma_r - \sigma_\theta)}{r} + f_\phi = 0, \tag{2}$$

where σ_r, σ_θ and f_ϕ are radial, circumferential stresses and the Lorentz's force respectively. The governing electrodynamics Maxwell equations for a perfectly conducting, elastic body [1] are given by

$$\vec{J} = Curl\vec{h}, \quad Curl\vec{e} = -\mu\frac{\partial\vec{h}}{\partial t}, \quad div\vec{h} = 0, \quad \vec{e} = -\mu\left(\frac{\partial U}{\partial t} \times \vec{H}\right), \quad \vec{h} = Curl(\vec{U} \times \vec{H}), \tag{3}$$

where $\vec{J}$, $\vec{e}$, $\vec{h}$ and $\vec{U}$ are electric current density vector, perturbation of electric field vector, perturbation of magnetic field vector and displacement vector respectively.

Imposing a magnetic field vector $\vec{H} = (0, 0, H_\phi)$ in spherical coordinate (r, θ, ϕ) system to Eq. (3) yields

$$\vec{U} = (u, 0, 0), \quad \vec{e} = -\mu(r)\left(0, H_\phi\frac{\partial u}{\partial t}, 0\right), \tag{4a}$$

$$\vec{h} = (0, 0, h_\phi), \quad \vec{J} = \left(0, -\frac{\partial h_\phi}{\partial r}, 0\right), \quad h_\phi = -H_\phi\left(\frac{\partial u}{\partial r}, \frac{2u}{r}\right). \tag{4b}$$

Then the Lorentz's force can be written as

$$f_\phi = \mu(r) \times (\vec{J} \times \vec{h}),$$

$$f_\phi = \mu(r)H_\phi^2\frac{\partial}{\partial r}\left(\frac{\partial u}{\partial r} + \frac{2u}{r}\right), \tag{5}$$

where $\mu(r)$ is the magnetic permeability. Substituting radial and circumferential stresses from Eqs. (1a) and (1b) and f_ϕ from Eq. (5) into equilibrium Eq. (2) the following differential equation is obtained

$$c_1\frac{\partial^2 u}{\partial r^2} + c_2\frac{\partial u}{\partial r} + c_3 u + c_4 = 0, \tag{6}$$

where coefficients c_1, c_2, c_3 and c_4 are written as follows:

$$\begin{aligned}
&c_1 = r^2, \\
&c_2 = (JI)r, \\
&c_3 = KI, \\
&c_4 = -IE_0\left[3(1+v)\beta\alpha_0 r^{\beta+1}T_0 + (1-v)r^2\frac{d\varepsilon_r^c}{dr} + 2vr^2\frac{d\varepsilon_\theta^c}{dr} + (\beta(1-v) + 2(1-2v))r\varepsilon_r^c + (2v(\beta+2)-2)r\varepsilon_\theta^c\right], \\
&I = \frac{1}{E_0(1-v) + \mu_0 H_\phi^2(1+v)(1-2v)}, \\
&J = E_0(1-v)(\beta+2) + 2\mu_0 H_\phi^2(1+v)(1-2v), \\
&K = 2E_0(v(\beta+1)-1) - 2\mu_0 H_\phi^2(1+v)(1-2v).
\end{aligned} \tag{7}$$

ε_r^c and ε_θ^c on the right hand side of the non-homogeneous coefficient c_4 are time, temperature and stress dependent.

3.1. Magnetothermoelastic analysis of FGM spheres

Ignoring the creep strain terms in non-homogeneous coefficient c_4 then differential Eq. (4) is a second order Ordinary differential equation (ODE) with variable coefficients the solution of which gives the thermoelastic stresses. A semi-analytical method [15] for solution of this differential equation has been employed. In this method the solution domain is divided into some finite divisions as shown in Fig. 1.

The coefficients of Eq. (4) are evaluated at $r^{(k)}$, mean radius of kth division and the ODE with constant coefficients valid only in kth sub-domain is rewritten as follows

$$\left(C_1^{(k)}\frac{d^2}{dr^2} + C_2^{(k)}\frac{d}{dr} + C_3^{(k)}\right)u^{(k)} + C_4^{(k)} = 0. \tag{8}$$

The coefficients of Eq. (8) are evaluated in each division in terms of constants and the radius of kth division.

The exact solution for Eq. (8) is written as follows

$$u^{(k)} = X_1^{(k)}\exp(\eta_1^{(k)}r^{(k)}) + X_2^{(k)}\exp\left(\eta_2^{(k)}r^{(k)}\right) - \frac{C_4^{(k)}}{C_3^{(k)}}, \tag{9}$$
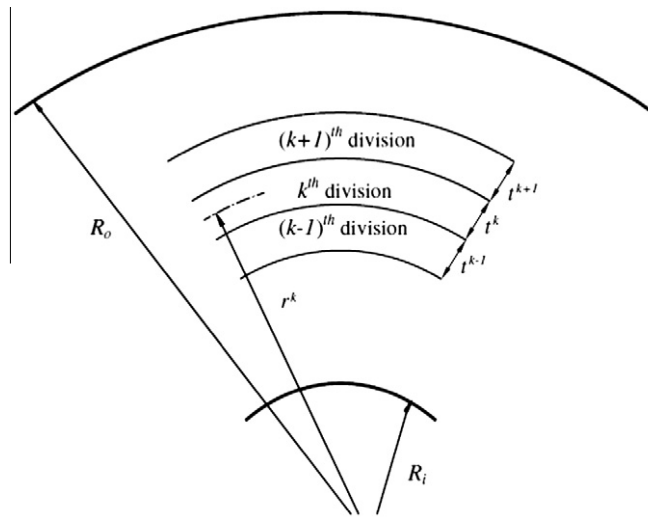
Fig. 1. Dividing radial domain into some finite sub-domains.

where

$$\eta_1^{(k)}, \eta_2^{(k)} = \frac{C_2^{(k)} \pm \sqrt{(C_2^{(k)})^2 - 4C_3^{(k)}C_1^{(k)}}}{2C_1^{(k)}}, \tag{10}$$

It is noted that this solution for Eq. (8) is valid in the following sub-domain

$$r^{(k)} - \frac{t^{(k)}}{2} \leqslant r \leqslant r^{(k)} + \frac{t^{(k)}}{2}, \tag{11}$$

where $t^{(k)}$ is the thickness of kth division and $X_1^{(k)}$, $X_2^{(k)}$ are unknown constants for kth division.

The unknowns $X_1^{(k)}$ and $X_2^{(k)}$ are determined by applying the necessary boundary conditions between two adjacent sub-domains. For this purpose, the continuity of the radial displacement u as well as radial stress σ_r is imposed at the interfaces of the adjacent sub-domains. These continuity conditions at the interfaces are

$$u^{(k)}\big|_{r=r^{(k)}+\frac{t^{(k)}}{2}} = u^{(k)}\big|_{r=r^{(k+1)}-\frac{t^{(k+1)}}{2}},$$
$$\sigma_r^{(k)}\big|_{r=r^{(k)}+\frac{t^{(k)}}{2}} = \sigma_r^{(k)}\big|_{r=r^{(k+1)}-\frac{t^{(k+1)}}{2}}. \tag{12}$$

And global boundary conditions are

$$\sigma_r = -P \text{ at } r = r_i,$$
$$\sigma_r = 0 \text{ at } r = r_o. \tag{13}$$

The continuity conditions Eq. (12) together with the global boundary conditions Eq. (13) yield a set of linear algebraic equations in terms of $X_1^{(k)}$ and $X_2^{(k)}$. Solving the resultant linear algebraic equations for $X_1^{(k)}$ and $X_2^{(k)}$, the unknown coefficients of Eq. (9) are calculated. Then, the displacement component u and the stresses are determined in each radial sub-domain. Increasing the number of divisions improves the accuracy of the results.

Thermo-elastic stresses obtained from this semi-analytical solution are shown in Figs. 2–4.

From thermo-elastic analysis the material identified by $\beta = 2$ in which the maximum effective stress distribution will occur throughout the thickness of the FGM sphere is selected for time-dependent stress redistribution analysis. Time-dependent solution can be done for all cases, however we have reported our results for the case $\beta = 2$ in this study.

3.2. Time-dependent magnetothermoelastic creep modeling of FGM spheres

For time-dependent creep analysis the creep strains in coefficient C_4 must be considered. Creep strains are time, temperature and stress dependent. Creep strain increments are related to the current stresses and the material uni-axial creep behavior by the well known Prandtl–Reuss relation. For problems of spherical symmetry these relations are

$$\Delta\varepsilon_r^c = \frac{\Delta\varepsilon_c}{\sigma_e}[\sigma_r - \sigma_\theta],$$
$$\Delta\varepsilon_\theta^c = \Delta\varepsilon_\phi^c = -\frac{\Delta\varepsilon_r^c}{2}, \tag{14}$$
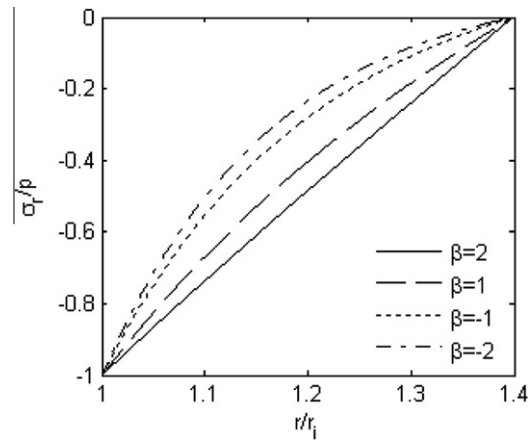
Fig. 2. Initial magnetothermoelastic radial stresses at zero time in the FGM sphere for $\beta = -2, -1, 1, 2$.
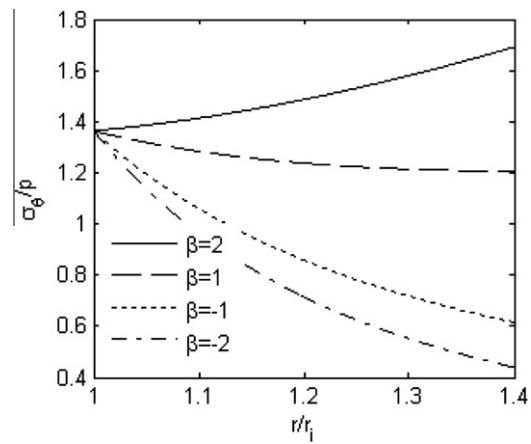

Fig. 3. Initial magnetothermoelastic circumferential stresses at zero time in the FGM sphere for $\beta = -2, -1, 1, 2$.
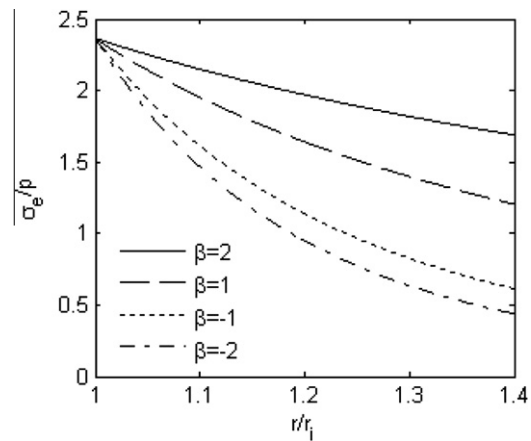

Fig. 4. Initial magnetothermoelastic effective stresses at zero time in the FGM sphere for $\beta = -2, -1, 1, 2$.

where $\Delta\varepsilon_r^c$ and $\Delta\varepsilon_\theta^c, \Delta\varepsilon_\phi^c$ are radial and circumferential creep strain increments, $\Delta\varepsilon_c$ and σ_e are equivalent creep strain increment and equivalent stress respectively. These equivalent or effective variables considering the spherical symmetry are defined as follows:

$$\Delta\varepsilon_c = |\Delta\varepsilon_r^c|,$$
$$\sigma_e = |\sigma_r - \sigma_\theta|, \tag{15}$$

The material creep constitutive model is Norton's law written as

$$\dot{\varepsilon}_e^c = B(r)\sigma_e^{n(r)},$$
$$B(r) = b_0 r^{b_1}. \tag{16}$$

Eqs. (14)–(16) in conjunction with differential equation (6) are used in a numerical procedure based on the Mendelson's method of successive elastic solution [16] or Harry Kraus [17] method of initial strains, to obtain history of stresses and deformations during creep evolution.

3.2.1. Numerical procedure to obtain history of stresses and strains

It was shown that creep strains and their derivatives are involved in non-homogenous part of differential Eq. (4) c_4. Immediately after loading the creep strains are zero and the solution is an elasticity problem. To solve differential Eq. (4) for long time after loading, method of successive elastic solution is used. Step by step procedure is explained in details as follows:

(1) An appropriate time increment must be selected for timing steps. In this study $\Delta t_i = 100000$ Sec is selected. The total time is the sum of time increments as the creep process progresses in time. For the ith timing step the total time is

$$t_i = \sum_{k=1}^{i-1} \Delta t_k + \Delta t_i. \tag{17}$$

(2) Initial values of $\Delta\varepsilon_{r,ij}^c = -0.0001$ are assumed at all division points (j) for ith timing step. These are added to the accumulated creep strains obtained from the previous timing step at all division points throughout the radius of the sphere

$$\varepsilon_{r,ij}^c = \sum_{k=1}^{i-1} \Delta\varepsilon_{r,kj}^c + \Delta\varepsilon_{r,ij}^c,$$
$$\varepsilon_{\theta,ij}^c = \sum_{k=1}^{i-1} \Delta\varepsilon_{\theta,kj}^c + \Delta\varepsilon_{\theta,ij}^c, \tag{18}$$
$$\Delta\varepsilon_{\theta,ij}^c = \Delta\varepsilon_{\phi,ij}^c = -\frac{\Delta\varepsilon_{r,ij}^c}{2},$$

where incompressibility condition is used to obtain tangential creep strain increments.

(3) With the assumed distribution for creep strain increments differential equation (6) can now be solved like thermoelastic solution and therefore the initial estimates of displacements and then current stresses are calculated.

(4) Effective Von Mises stresses are then calculated at all division points as

$$\sigma_{e,ij} = |\sigma_{r,ij} - \sigma_{\theta,ij}|. \tag{19}$$

(5) Effective creep strain increments are then calculated at all division points (j) for ith timing step using Norton's creep constitutive model as follows

$$\Delta\varepsilon_{c,ij} = \left[B(r_j)\sigma_{e,ij}^{n_0}\right]\Delta t_i,$$
$$B(r_j) = b_0 r_j^{b_1}. \tag{20}$$

(6) From Prandtl–Reuss equation new values of creep strain increments are obtained

$$\Delta\varepsilon_{r,ij}^{c,new} = \frac{\Delta\varepsilon_{c,ij}}{\sigma_{e,ij}}[\sigma_{r,ij} - \sigma_{\theta,ij}],$$
$$\Delta\varepsilon_{\theta,ij}^{c,new} = \Delta\varepsilon_{\phi,ij}^{c,new} = -\frac{\Delta\varepsilon_{r,ij}^{c,new}}{2}. \tag{21}$$

(7) These new obtained values for creep strain increments are then compared with the initial estimated values for the convergence of the procedure. If convergence is satisfied, time is advanced one increment and the procedure is repeated for the new time increment from step one. If convergence is not satisfied, these new obtained values of creep strain increments will be considered as initial values and the procedure will be repeated from step 2 until convergence is obtained.
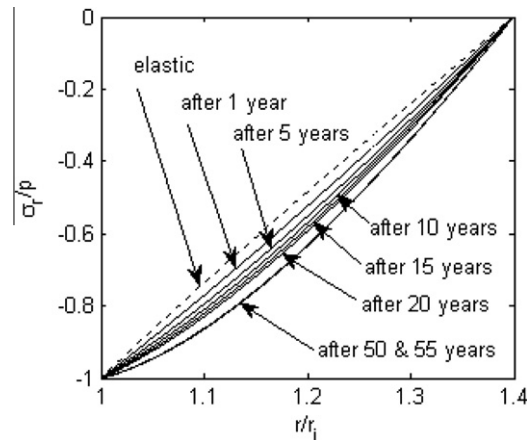
Fig. 5. History of magnetothermoelastic creep radial stress in the FGM sphere from its initial elastic at zero time up to 55 years for the case β = 2.
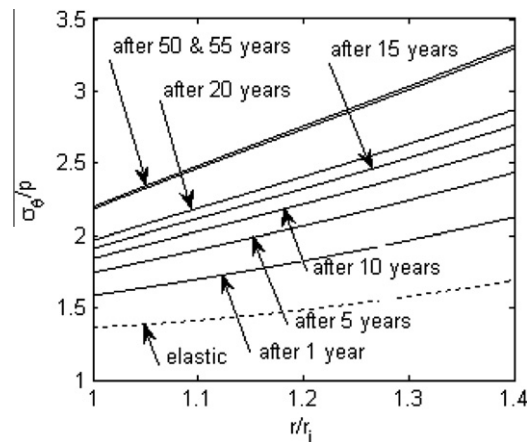

Fig. 6. History of magnetothermoelastic creep circumferential stress in the FGM sphere from its initial elastic at zero time up to 55 years for the case β = 2.

From the above numerical procedure history of stresses, strains and effective creep strain rates of FGM sphere are obtained and illustrated in Figs. 5–10.

4. Results and discussion

Initial magnetothermoelastic radial stresses at zero time are shown in Fig. 2. The boundary conditions for radial stresses at the inner and outer surfaces of the sphere are satisfied for all material properties. There are not significant differences among radial stresses for all material properties therefore the material power index β has no significant effect on radial stresses. Tangential magnetothermo-elastic stresses at zero time are shown in Fig. 3 for different material properties. They are tensile throughout thickness and are increasing by increasing the material power index β. The material power index β has a significant effect on circumferential stress distribution.

Fig. 4 shows the effective stress distribution throughout thickness for all cases of material properties. Since effective stresses of Von Mises and Tresca are the same in spherical symmetry $\sigma_{e,ij} = |\sigma_{r,ij} - \sigma_{\theta,ij}|$ and effective stresses are indeed twice as the maximum shear stresses ($\sigma_e = 2\tau_{\max}$) therefore it is clear from Fig. 4 that the material with β = 2 has the maximum shear stress distribution throughout thickness. The minimum shear stress distribution belongs to material identified by β = −2. History of stresses and strains during creep process is investigated for the material identified by β = 2.

History of creep stresses for material identified by β = 2 are shown in Figs. 5–7. Fig. 5 shows radial stress redistribution in a FGM sphere from its initial elastic up to 55 years. It is clear from this figure that radial stress redistribution is not really significant however it changes in time with a decreasing rate so that after 50 years it becomes steady so that no distinction can be identified between radial stresses at 50 and 55 years. History of circumferential stress is shown in Fig. 6. Major redistribution has occurred for circumferential stress. Circumferential stress is also increasing in time with a decreasing rate so
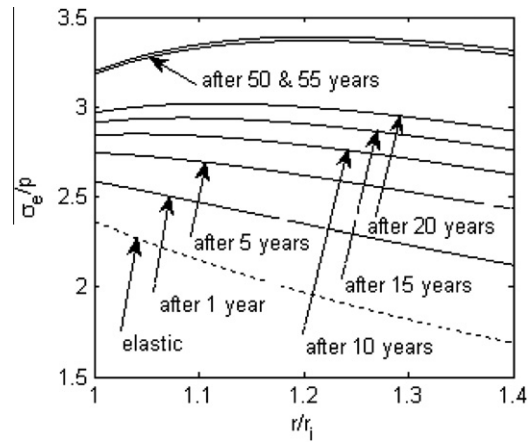
Fig. 7. History of magnetothermoelastic creep effective stress in the FGM sphere from its initial elastic at zero time up to 55 years for the case $\beta = 2$.
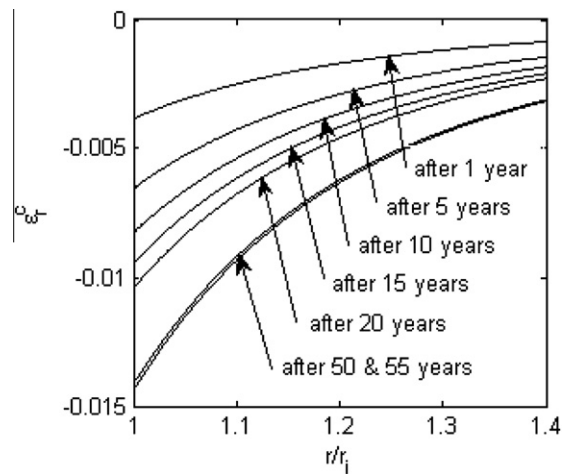

Fig. 8. History of radial creep strain in the FGM sphere from its initial elastic up to 55 years for the case $\beta = 2$.
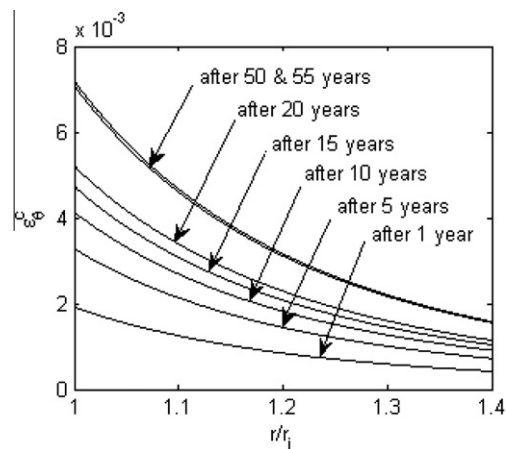

Fig. 9. History of circumferential creep strain in the FGM sphere from its initial elastic up to 55 years for the case $\beta = 2$.
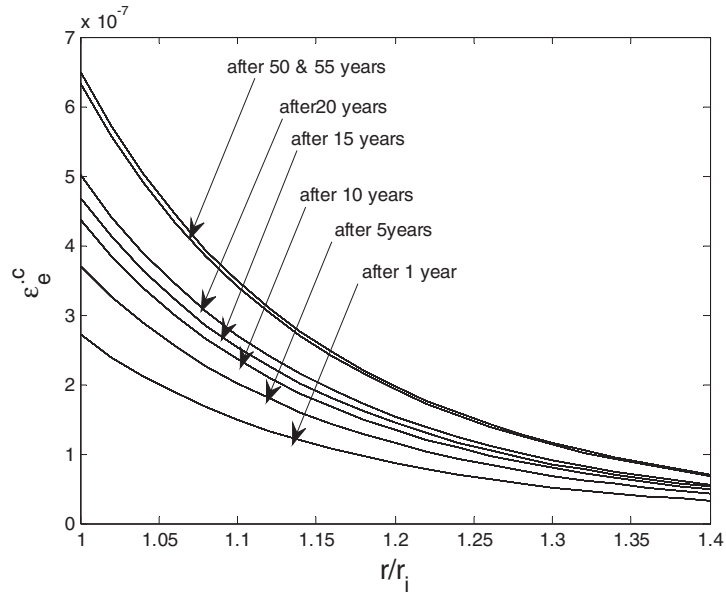
Fig. 10. History of effective creep strain rates in the FGM sphere from its initial elastic up to 55 years for the case $\beta = 2$.

that after 50 years it becomes steady so that no distinction can be identified between circumferential stresses at 50 and 55 years. Effective stress redistribution is shown in Fig. 7. Since the effective stress is twice as the maximum shear stress at each point throughout thickness, therefore the maximum shear stress distribution is increasing with time throughout thickness of the vessel during creep process. It can also been concluded from the history of effective stress that almost after 50 years time-dependent solution approaches to the steady state condition because no distinction can be reported between effective stresses at 50 and 55 years. History of creep strains are shown in Figs. 8 and 9. The absolute value of radial and circumferential creep strains is increasing with a decreasing rate so that after almost 50 years they become steady and no distinction can be identified between creep strains at 50 and 55 years.

From Eq. (20) effective creep strain rate histories are shown in Fig. 10. It is clear that effective creep strain rates are changing with time with a decreasing rate and finally converge to the steady state condition. It is also concluded that the maximum effective creep strain rates are located at the inner surface of the sphere while the minimum rates are located at the outer surface of the vessel.
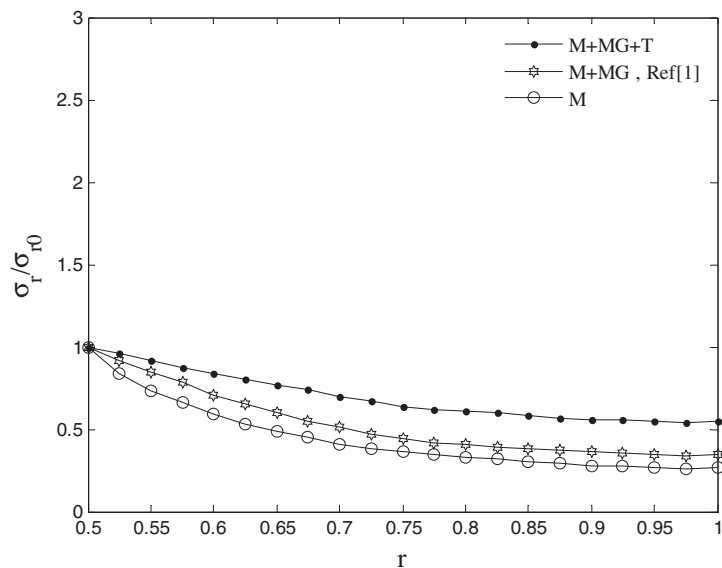

Fig. 11. Effect of mechanical, magnetic and thermal fields on radial stress considering geometry and material properties of Ref [1].

There is no solution available in the literature for magnetothermoelastic creep analysis of spheres so we cannot validate with other references. However considering geometry and material property of Ref. [1] the effect of mechanical, magnetic and thermal field for elastic radial stress has been depicted in Fig. 11. It has been found that the minimum radial stress distribution belongs to mechanical loading. Adding magnetic and thermal loads will increase radial stress distribution. If we ignore the effect of thermal field the result is validated with Ref. [1].

5. Conclusion

A semi-analytical solution in conjunction with the Mendelson's method of successive elastic solution has been successfully employed to obtain history of magnetothermoelastic creep stresses, strains and effective creep strain rate. History of stresses, strains and effective creep strain rate are presented from their initial elastic values at zero time up to 55 years. It has been concluded from the history of stresses and strains that after almost 50 years the time-dependent solution approaches to the steady state condition when there is no distinction between stresses and strains at 50 and 55 years. It has also been found that the maximum effective creep strain rates are located at the inner surface of the FGM sphere while the minimum rates are located at the outer surface of the vessel. The results are validated for elastic radial stresses considering mechanical and magnetic fields.

References

[1] H.L. Dai, Y.M. Fu, Magnetothermoelastic interactions in hollow structures of functionally graded material subjected to mechanical load, Int. J. Press. Ves. Pip. 84 (2007) 132–138.
[2] A. Ghorbanpour, M. Salari, H. Khademizadeh, A. Arefmanesh, Magnetothermoelastic stress and perturbation of magnetic field vector in a functionally graded hollow sphere, Arch. Appl. Mech. (2010) 189–200.
[3] N. Tutuncu, B. Temel, A novel approach to stress analysis of pressured FGM cylinders, disks and spheres, Compos. Struct. 91 (2009) 385–390.
[4] O. Yoshihiro, T. Yoshinobu, The transient piezothermoelastic analysis for a functionally graded thermopiezoelectric hollow sphere, Compos. Struct. 81 (2007) 540–549.
[5] L.H. You, H. Ou, Z.Y. Zheng, Creep deformation and stresses in thick-walled cylindrical vessels of functionally graded materials subjected to internal pressure, Compos. Struct. 78 (2007) 285–291.
[6] T. Singh, V.K. Gupta, Effect of anisotropy on steady state creep in functionally graded cylinder, Compos. Struct. 93 (2011) 747–758.
[7] A. Loghman, N. Shokouhi, Creep damage evaluation of thick-walled spheres using a long-term creep constitutive model, J. Mech. Sci. Tech. 23 (2009) 2577–2582.
[8] R.W. Evans, J.D. Parker, B. Wilsher, The Theta projection concept a model based approach to design and life extention of engineering plant, Int. J. Press. Ves. Pip. 50 (1992) 60–147.
[9] A.S. Khan, O. Lopez-Pamies, Time and temperature dependent response and relaxation of a soft polymer, Int. J. Plastic. 18 (2002) 1359–1372.
[10] A. Loghman, M.A. Wahab, Creep damage simulation of thick-walled tubes using the theta projection concept, Int. J. Press. Ves. Pip. 67 (1996) 105–111.
[11] R.G. Sim, R.K. Penny, Plane strain creep behaviour of thick-walled cylinders, Int. J. Mech. Sci. 13 (1971) 987–1009.
[12] Fu-Zhen Xuan, Jian-Jun Chen, Zhengdong Wang, Shan-Tung Tu, Time-dependent deformation and fracture of multi-material systems at high temperature, Int. J. Press. Ves. Pip. 86 (2009) 604–615.
[13] Y.Y. Yang, Time-dependent stress analysis in functionally graded material, Int. J. Solid. Struct. 37 (2000) 7593–7608.
[14] A. Loghman, A. Ghorbanpour Arani, S. Amir, A. Vajedi, Magnetothermoelastic creep analysis of functionally graded cylinders, Int. J. Press. Ves. Pip. 87 (2010) 389–395.
[15] S.A. Hosseini Kordkheili, R. Naghdabadi, Thermo-elastic analysis of a functionally graded rotating disk, Compos. Struct. 79 (2007) 508–516.
[16] A. Mendelson, Plasticity Theory and Applications, Macmillan, New York, 1968.
[17] H. Kraus, Creep Analysis, John Wiley & Sons, New York, 1980.